

Monitoring riverine sediment fluxes during floods: new tools and methods

Eric LAJEUNESSE

Institut de Physique du Globe - Sorbonne Paris Cité
Equipe de Dynamique des fluides géologiques
1 rue Jussieu, 75238 Paris cedex 05, France

Christophe DELACOURT

Institut Universitaire Européen de la Mer
Université de Bretagne Occidentale
Domaines Océaniques - UMR 6538, Place Copernic, 29280-PLOUZANE, France

Pascal ALLEMAND

Laboratoire de Géologie de Lyon
Université Lyon 1 et ENS-Lyon
2, rue Raphaël Dubois, 69622 Villeurbanne cedex, France

Angela LIMARE

Institut de Physique du Globe - Sorbonne Paris Cité
Equipe de Dynamique des fluides géologiques
1 rue Jussieu, 75238 Paris cedex 05, France

Céline DESSERT

Institut de Physique du Globe - Sorbonne Paris Cité
Equipe de Géochimie et Cosmochimie
1 rue Jussieu, 75238 Paris cedex 05, France

Jérôme AMMANN

Institut Universitaire Européen de la Mer
Université de Bretagne Occidentale
Domaines Océaniques - UMR 6538, Place Copernic, 29280-PLOUZANE, France

Philippe GRANDJEAN

Laboratoire de Géologie de Lyon
Université Lyon 1 et ENS-Lyon
2, rue Raphaël Dubois, 69622 Villeurbanne cedex, France

ABSTRACT: We report a new methodology to estimate the impact of extreme events on sediment transport in rivers. Our approach relies on two complementary instruments developed and tested during a 1.5 years field survey performed from June 2007 to January 2009 on the Capesterre river located on Basse-Terre island (Guadeloupe archipelago, Lesser Antilles Arc). The first one, CAPMES, performs real-time in-situ measurements of the water stage together with the concentration and the average grain size of suspended silts and sand particles. The second one, DRELIO, acquires high resolution stereophotogrammetric images of river beds used to compute DEMs and to

estimate how flash floods impact the granulometry and the morphology of the river. The combined use of these two instruments provides a platform of investigation of the erosive impact of extreme events in rivers exposed to the risk of flash floods. This platform can be used for either field campaigns of limited duration or long-term surveys of riverine sediment transport.

1 INTRODUCTION

A series of recent studies have underlined that the volume of sediment exported from a watershed is dramatically increased during extreme climatic events, such as storms, tropical cyclones and hurricanes (Dadson et al. 2004; Hilton et al. 2008). The exceptionally high rainfall rates reached during these events trigger runoff and landsliding which destabilize slopes and accumulate a significant amount of sediments in flooded rivers (Gabet et al., 2004; Lin et al., 2008). This observation raises the question of the role of extreme climatic events in setting the denudation rate and the morphology of watersheds. Moreover infrastructures and populations concentrated around rivers are very vulnerable to erosion and sediment transport associated with flash flood phenomena, and require constraints on frequency and timing of events and their expected impact.

Addressing these challenges requires instruments and methodologies capable of 1) performing long surveys with minimum human intervention and 2) acquiring data even under extreme climatic events. However most conventional sediment monitoring techniques rely on manual measurements which cannot be performed during extreme events (Garcia, 2006). As a result, the great majority of data available in the literature cannot be used to investigate the erosive impact of flash floods (Summerfield et al., 1994; Turowski et al., 2010). Moreover these datasets mostly focus on the solute and suspended load thus ignoring bedload despite its importance (Meunier et al., 2006; Liu et al., 2008; Lajeunesse et al., 2010).

In this paper, we present a new methodology aimed at estimating the impact of extreme events on sediment transport in rivers. Our approach relies on the use of two instruments. The first one is an in-situ optical instrument capable of measuring both the water level and the concentration of suspended matter in rivers with a time step going from one measurement every hour at low flow to one measurement every 2 minutes during a flood. The second instrument is a remote controlled helicopter used to acquire stereophotogrammetric images of river beds with centimetric spatial resolution. The comparison of images acquired before and after a major event allows one to estimate its impact on the granulometry and the morphology of the river bed. These two instruments were tested during a 1.5 years field survey performed from June 2007 to January 2009 on the Capesterre river on Basse-Terre island (Guadeloupe archipelago, Lesser Antilles Arc) chosen for its torrential hydrologic regime characterized by abrupt flow rate variations due to tropical storms and hurricanes. We show that they enable the acquisition of data which better constrain the dynamics of sediment transport during floods.

2 DESCRIPTION OF THE FIELD SITE: THE CAPESTERRE RIVER

The Capesterre river is located on Basse-Terre, a volcanic island belonging to the archipelago of Guadeloupe located in the Lesser Antilles arc. The latter results from the ongoing subduction of the Atlantic plate under the Caribbean plate (Feuillet et al., 2001). A recent investigation of the chemistry of dissolved and suspended load provided the first estimate of the Lesser Antilles arc chemical weathering rates with values of 100 to 120 $\text{t.km}^2.\text{y}^{-1}$ (Rad et al., 2006; Gaillardet et al., submitted). Mechanical erosion rates, deduced from geochemical mass balance between mean unaltered rock and dissolved and solid loads, were found to range from 800 to 4000 $\text{t.km}^2.\text{y}^{-1}$, that is between 300 and 1500 mm/ky. If confirmed, such erosion rates would place the Antilles among the fastest eroding places in the world well above Ganges or Brahmaputra catchments where denudation rates are respectively 273 and 688 mm/ky (Galy and France-Lanord, 2001).

The Capesterre river drains a watershed of 37.3 km^2 located on the windward side of the active Soufrière volcano (Figure 1a). Its length is 18.6 km with headwaters at 1300 m, discharging into the sea at the Capesterre village. Capesterre was chosen because of its flashy discharge regime (Fig. 1b). Moreover, its flow rate is monitored by the Direction Régionale de l'Environnement (DIREN) with a data base covering more than 10 years and the depth-discharge relationship is well known. Capesterre watershed, mainly

composed of lava and pyroclastic flows aged from 600 to 400 ky (Samper et al., 2007), is characterized by rather thin soils, typically ranging from 0.5 to 2 meters. Capesterre is a bedrock river partially covered by a thin alluvial cover the thickness of which can increase locally likely due to overwhelming sediment supply from adjacent hillslopes, gullies or tributaries. Close to the sea, slopes become gentler and the river bed undergoes a bedrock to alluvial transition. The granulometry of the river was characterized by applying the surface count (Wolman grid-by-number) technique on 5 sites located at regular intervals along the river (Wolman, 1954). The results indicate that the median diameter is comprised between 30 and 250mm and reveals the presence of numerous metric size blocks. The sand fraction is very small (less than 0.2%) except in the immediate vicinity of the sea. These characteristics are shared by the majority of Basse-Terre rivers (Chatanantavet et al., 2007; Chatanantavet et al., 2010).

Climate is tropical with high temperatures (24-28 °C) and an average annual precipitation rate of about 5200 mm/y. The hydrologic regime is torrential: flow rate is characterized by abrupt variations due to tropical rains. Storms and hurricanes are particularly frequent during the rainy season from June to January (see Figure 1 b) with maximum daily precipitation rates reaching up to 590 mm/day.

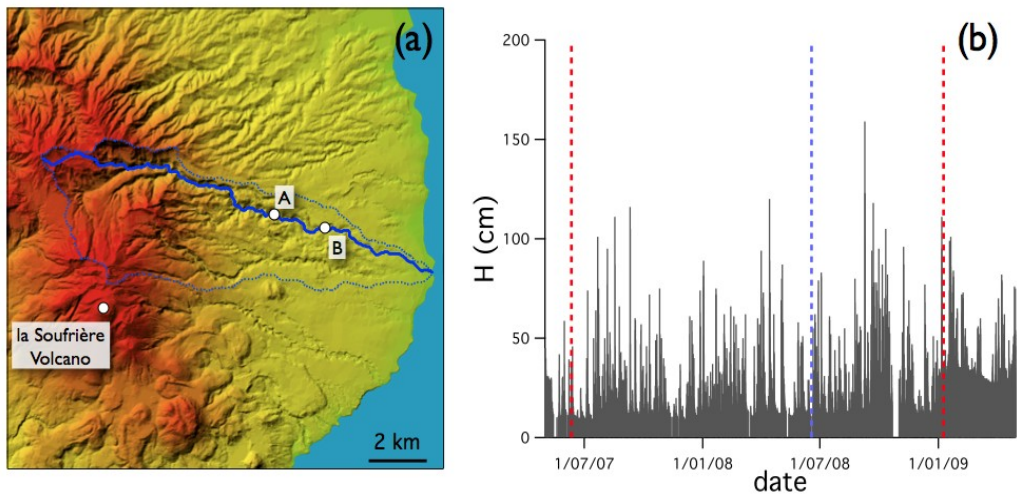


Figure 1 (a) Topographic map of the Capesterre watershed. The frontiers of the watershed and the Capesterre river are indicated by respectively the dotted and the solid curve. The suspended load sensor is located on site A while the drone imaging method was tested on site B. (b) Variations of the water flow depth in the Capesterre river on site A between June 2007 and June 2009 (data by courtesy of the Direction Régionale de l'Environnement). The dates of image acquisition (06/11/2007 and 01/09/2009) are indicated by the two red vertical dotted line. The installation date of the suspended load sensor (06/18/2008) is indicated by the vertical dotted blue line

3 SUSPENDED LOAD MONITORING

The method developed to monitor the suspended load in rivers makes use of a LISST-25X (Laser In-Situ Scattering and Transmissometry) sensor developed by Sequoia Scientific, Inc. This instrument determines the volumetric concentration of suspended particles in two size classes (1.25-63 μm and 63-250 μm) from their characteristic multi-angle forward scattering of an infrared laser ray. The LISST-25X also measures the Sauter mean diameter (the ratio of total volume to total area of particles) which can be used as a proxy for the mean grain size. The measurement of the sediment size and granulometry marks a departure from the more conventional light-source-detector technology employed in previous optical sediment sensors, like turbidimeters (Agrawal and Pottsmith, 2000). The LISST-25X is able to detect particles over a size range of 1.25 to 250 μm . However too many particles outside this range will cause measurement errors. Moreover detection operates in a volumetric concentration range from 10^{-2} to 10^2 ppm, corresponding to mass concentrations from 10^{-4} to 1 g/l. Higher concentrations could be measured by reducing the optical path of the sensor or by diluting the sample in line.

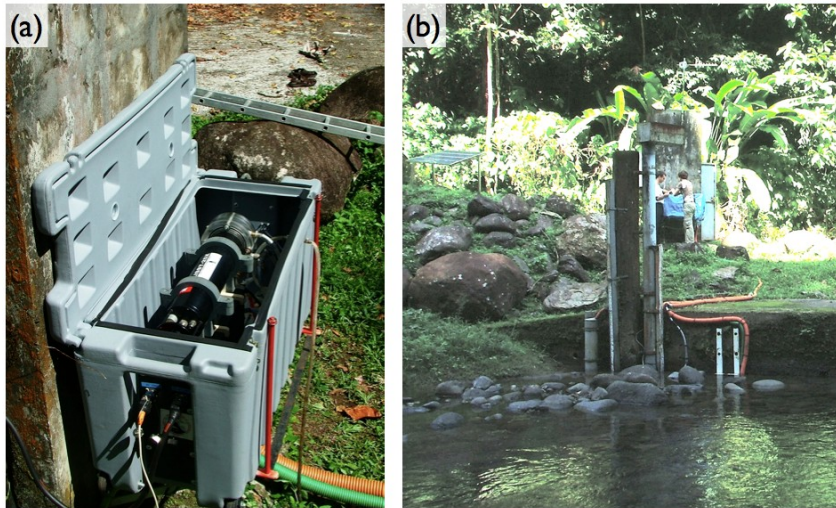


Figure 2 (a) Picture of CAPMES showing the LISST-25 X and the measurement cell. (b) Image of the field test site on the Capesterre river. The sensor and the data logger are located at about 8 meters away from and 1.5 meter above the river bed while the pump is submersed into the stream

Although LISST sensors have already been tested for in-situ monitoring of suspended load in rivers (Melis et al., 2003; Topping et al., 2004), they have not been used to monitor sediment transport during floods. After a series of field tests performed in the Capesterre river in 2007, it became obvious that the LISST-25X had to be included in a more complex hydraulic and electronic system in order to become a stand-alone instrument capable of 1) performing long surveys with minimum human intervention and 2) acquiring data even under extreme climatic events. To this end, we integrated the suspended load sensor in a hydraulic and electric system, controlled by a data logger. The resulting instrument, called CAPMES, is designed to comply with demands as discussed below.

To avoid destruction of the apparatus during flash floods, the suspended sediments sensor cannot be installed directly in the river bed but needs to be placed in a safe location along the banks. CAPMES is therefore equipped with a pump, installed in the river, which transfers water from the river into a measurement cell implemented onto the LISST-25 X (see Figure 2). In this way, only the pump, which is rather cheap, is exposed to possible destruction during a large flood. The pump needs to be powerful enough to guarantee that both the concentration and the granulometry of the suspended particles transported to the measurement cell are representative of the suspended load in the river. We used a Barwig 12V/50W submersible pump which provides a discharge of 4l/min. Laboratory tests performed with suspensions of glass beads showed that such a discharge is enough to keep all the particles suspended in a 10m long and 10mm diameter tube with a 2.5m level difference between the hose and the measurement cell.

The LISST 25 X sensor needs to be regularly cleaned and calibrated. This is achieved by means of a second pumping device connected to a clean water tank, used to inject clean water into the measurement cell at regular time intervals set by the user (once a day in our case). A first series of injections are performed to clean the measurement cell. Once this is done, the measurement cell is filled with clean water and the LISST is calibrated by measuring the background light scattering of the optical surfaces. A water presence sensor (Honeywell) is used to prevent cleaning and calibration of the LISST if the clean water tank is empty.

To increase the energetic autonomy of the instrument, we removed the four 9V internal batteries powering the LISST 25 X. Instead, we used an available pin of the LISST cable to connect the instrument to external batteries continuously recharged by a solar panel.

In order to save energy and disk space, it is necessary to adapt the measurement time step to the state of the river. This is achieved by using a hydrostatic level sensor (GEMS Sensors), placed in the river close to the pump hose, which measures the water level every minute. When the water level H exceeds a threshold value H_{start} , a flood is detected and the measurement frequency is set to a high value, F_{flood} which can

reach up to 1 measurement every 2 minutes. This measurement frequency is conserved until H falls below a value H_{stop} . H_{start} and H_{stop} are set by the user and are not necessarily equal. In between floods, the measurement frequency is set to a low value F_{low} chosen by the user. During our field survey on the Capesterre river, we used $H_{\text{start}} = 50$ cm, $H_{\text{stop}} = 40$ cm, $F_{\text{flood}} = 1$ measurement every 2 minutes and $F_{\text{low}} = 1$ measurement every hour.

The two pumping devices, the cleaning water circuit, the pressure sensor and the LISST 25X are controlled by a data logger which also stores the data. The data logger is based on a Persistor CF2 that incorporates elaborate control and data logging capabilities into a compact and very low-power module (less than 0.5 watt). A standard CompactFlash header is built onto the CF2. The memory card contains a DOS like operating system allowing it to launch a datalogging program that can be loaded from the computer through a serial interface. The datalogger controls the LISST-25X instrument through a receive and transmit RS232 channel. It also controls a relay card that supplies power to the two pumps. The signals from the two sensors are connected to two 12 bit AD input channels. Data files (containing water level, size and concentration of the particles) together with log files (containing information about the reboot time and the absence of water in the tank or in the river) are regularly saved on the compact flash disk.

The instrument autonomy is limited mainly by the clean water tank capacity. In our case, the cleaning and background procedure consumes 1.6 L, meaning that for a 60 L tank, the instrument has an autonomy of about a month. Once in a month, a maintenance operation is required. It consists of collecting the data, refilling the clean water tank, checking the components according to a check list (LISST status, sensors levels, pumps and relays) and controlling CAPMES calibration and parameters..

4 DRELIO, A DRONE HELICOPTER DEDICATED FOR OBSERVATIONS OF THE ENVIRONMENT

Despite recent advances (Burtin et al., 2008; 2009), there is currently no instrument capable of continuous automated measurement of bedload transport. Bedload transport measurements are still based on direct measurements by an operator and cannot be performed during a flood for obvious safety reasons. This is why we chose to focus on an indirect methodology based on the acquisition of high resolution images with the goal of estimating the impact of floods on the river morphology and granulometry.

Images acquired before and after a flood are indeed essential synoptic data sets to measure the changes undergone by rivers. Volume of eroded or deposited sediment can be measured from Digital Elevation Models (DEM) calculated from stereoscopic images. Changes in granulometry measured from orthorectified-images can be used to estimate the maximum bed shear stress during a flood provided the resolution is high enough and images are taken shortly after the flood. These constraints can be met using the DRELIO system which is an autopiloted drone helicopter.

4.1 Description of the Drelion system

Although platforms such as kites, microlights and drones have been tested for surveying landslides (Casson et al., 2005), for mapping alpine rivers (Lejot et al., 2007) as well as for agricultural (Sugiura et al., 2005) and coastal applications (Delacourt et al., 2009), few of them have ever been used to monitor river sediment flux. The DRELIO system was developed to meet the constraints specifically associated to tropical external conditions namely dense vegetation, small takeoff area and steep-sided watersheds. Furthermore products derived in this study, including a multitemporal Orthorectified DEM and orthophotography, have not been calculated elsewhere.

The DRELIO system consists of 4 main parts (Figure 3) : a) the helicopter b) the payload for scientific sensors c) the on-board flight control system (FCS) and d) the ground control station (GCS) for mission planning and control. The helicopter is a Vario rigidified acrobatic thermic model. Rotation speed of blades has been reduced in order to limit vibrations and to increase flight stability. Despite this limitation, the maximum speed is $70 \text{ km}\cdot\text{h}^{-1}$. The total weight is 11 kg with a maximum payload of 6 kg.

The ground control station is connected to the on board flight control system. It pilots the acquisition instruments in terms of time of start and frequency of acquisition. A programmable autopilot, connected to an atmospheric pressure sensor, an inertial sensor, a geomagnetic direction sensor and a GPS, drives and stabilizes the helicopter. DRELIO is thus capable of fully automatic take-off, hovering, flight plan following and landing. Its integrated radio link allows data communication up to 60 km. Once a flight

plan is loaded, no ground communication is needed. This extends the range of operation beyond radio reach.

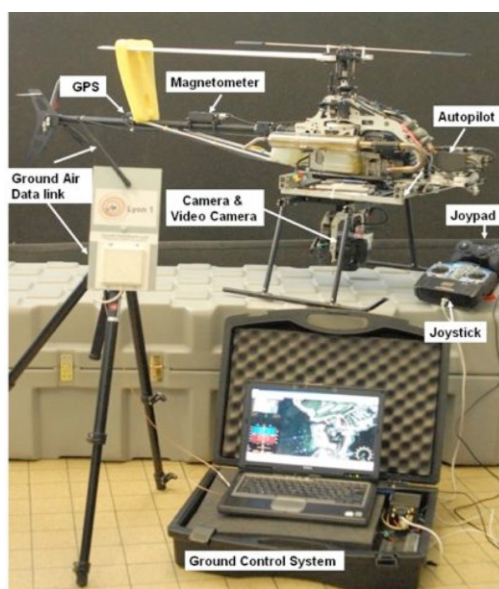


Figure 3 Technical configuration of DRELIO system. The DRELIO copter is equipped with position and attitude sensors (Magnetometer, GPS and pressure sensor not represented here) which inform the autopilot 100 times by second. The ground control system can be used to pilot DRELIO during a mission. It is mainly used to overload the path which DRELIO has to follow. DRELIO can perform a mission without any radio contact with the Ground Control System

The payload classically consists of a professional reflex camera installed under the helicopter. As the control station is linked to a GPS, series of specific photographs can be programmed in order to realize multitemporal comparisons from the same point and angle of view. A video camera installed on the view finder of the reflex camera transfers in real time to the ground the images visible through the reflex camera. This low resolution video is used only to control the swath coverage during the acquisition run. To reduce the number of images necessary to cover a given zone, lenses with a focal length smaller than or equal to 50 mm are used. Pixel size is from 1cm to 4cm with a focus length of 50mm and a flight altitude typically ranging from 50 to 200m. In that case, the swath width ranges from 50 to 200m.

Missions are best flown early in the morning or late in the evening when the sun is just under the horizon. Then, the light is homogeneous and the lack of shadows allows a good processing of images. Moreover, the period of dawn and twilight are characterized by low wind. If several missions are planned over the same area, they should be realized in the same illumination conditions.

The flight plan of DRELIO is first loaded in the autopilot from the ground station. The flight plan is made up of the position of points where DRELIO has to change its course, the landing location, the velocity between points and the emergency landing site in case of link break-off between the station and the helicopter. Before takeoff, DRELIO is verified according to a check list. Both mechanical, electronic and image systems are checked and verified. Then, the engine is started up. After the heating of the engine, the mission is launched by a start up order given to the software. At every moment, the flight can be controlled from a manned remote control if a problem is detected. Once the flight is over, the images are transferred from the camera to a computer in order to be inspected.

4.2 DEM and Ortho-images processing

Digital Elevation Models (DEMs) can be derived using photogrammetric techniques applied to two images of a stereoscopic pair, that are acquired over the same area from different view angles and/or different positions. This technique requires knowledge of the optical characteristics of the camera, and of

the position and orientation of the camera at the time of acquisition which are called external parameters. The optical characteristics of the camera are known either from the camera manufacturer or by measuring them before the mission (Kasser and Egels, 2002). The external parameters of the camera are defined for each image.

A DEM can be derived from stereoscopic images acquired by DRELIO using methods similar to those used in classical airborne missions, even if the calculation is more difficult. The first problem is to control and obtain a precise set of external parameters. In terms of altitude and orientation, the flight of DRELIO is not as stable as that of a plane. Moreover, GPS equipment on board of DRELIO does not give sufficiently accurate measurements with respect to the spatial resolution of the images. The external parameters of each image are thus poorly defined. The precision on these parameters is increased using ground control points (GCP) identified by red targets installed on the ground before acquisitions and geo-located by differential GPS with a precision of few centimeters. Using the absolute locations of these points and their positions on the images, minimization methods have been developed to increase the accuracy of the external parameters (Kasser and Egels, 2002). In the following step, the position of each point on the first image is associated with the position of the analogous point in the second image. The correspondence between the pixels of the two images is calculated by maximizing a correlation function (Casson et al., 2005; Delacourt et al., 2004) which is used to measure the shift between each point of the two images. Finally, the photogrammetric equations are applied to each pair of correlated points to determine their 3D coordinates (Kraus and Waldhäusl, 1994). Orthophotographs which are images corrected for geometrical and topographical distortions are then computed from the DEM and one of the images of the stereoscopic pair.

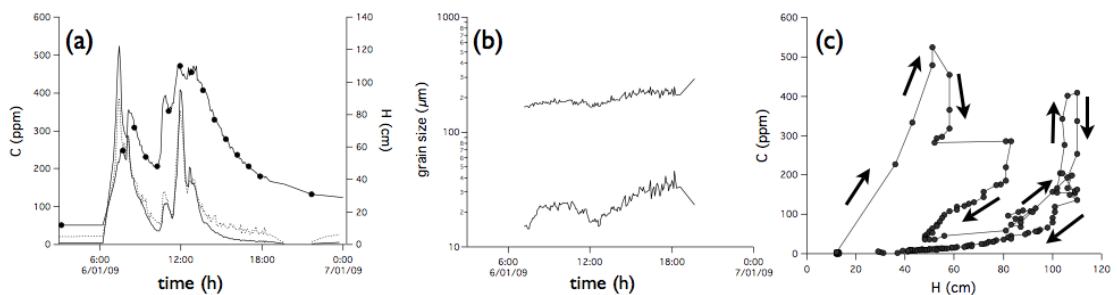


Figure 4 Data acquired by CAPMES during a flash flood on January 6th 2009. (a) Water flow depth (line with circles), volumetric concentration of suspended silt (solid line) and sand (dotted line) as a function of time; (b) Average grain size of silt and sand particles as a function of time; (c) Plot of silt concentration vs water level. Arrows indicate forward time

5 RESULTS

CAPMES was installed along the bank of the Capesterre river from June 20, 2007 to January 30, 2009. It continuously recorded the water depth and the suspended load concentration and granulometry, except for a period between september 19th and november 4th 2008 due to a failure of the solar panel. The site located on the Capesterre river was imaged by DRELIO in January 2008 and January 2009. Each time, more than 100 high resolution images covering a 300 m long reach along the river were taken from a height of 150m. The overlap of successive images was around 70% for each series. It was therefore possible to calculate DEM and ortho-images from the dataset of each mission. Several flash floods occurred during our survey. Although none of them was high enough to lead to important changes of the river bed, they allow us to illustrate the interest of our methodology.

Figure 4a shows data acquired by CAPMES during a typical flash flood which occurred on January 6th 2009. Before the flood, the water level in the river was 12 cm, which, according to the depth-discharge relationship, corresponds to a flow rate of about $1 \text{ m}^3\text{s}^{-1}$. At around 6 am GMT (2 am, local time), the water level started to rise, triggering an increase of the acquisition frequency to 1 measurement every 2 minutes. The water level reached a first peak at $H=83 \text{ cm}$ (about $28 \text{ m}^3\text{s}^{-1}$) after almost two hours. After a temporary decrease, the water level rapidly rose again until it reached a second peak at $H=110 \text{ cm}$ ($50 \text{ m}^3\text{s}^{-1}$) around noon GMT (8 am, local time). After this second peak, the water level slowly decreased back

to normal. The concentration of silt (grain size in the range 2.5-63 μm) and sand (grain size in the range 63-250 μm) particles, initially equal to zero, started to increase simultaneously with the water level. Their overall evolution reflects that of the water level with some differences. Interestingly, the first peak of suspended load concentration was reached about 40 minutes in advance of the first water level peak, whereas the second peak of suspended load concentration was reached about 10 minutes after the second water level peak. This observation points out the fact that the suspended load concentration is not a simple and direct function of the flow depth in the river. This is best evidenced by a plot of concentration vs water depth shown in figure 4 c which shows hysteretic behavior. This cannot be attributed to a change of grain size. Indeed, as shown on Figure 4 b, the average diameter of the silt and sand particles remained almost constant during the flood. As illustrated by this example, CAPMES enables the observation of the suspended load properties with an unprecedented resolution. The data acquired by CAPMES are thus likely to lead to new insights on the dynamics of sediment transport. Their detailed analysis goes beyond the scope of the present paper and will be the subject of a forthcoming paper.

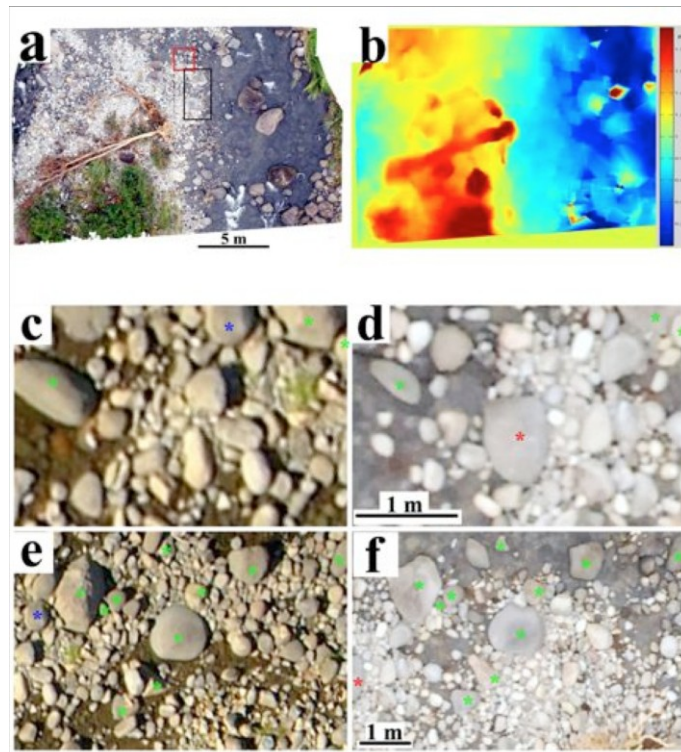


Figure 5 Example of ortho-images of a gravel bank of the Capesterre river showing the change of granulometry which occurred between January 2008 to January 2009. a) and b) General view and Digital Elevation Model of the studied gravel bank in 2009. The squares show the position of the high resolution ortho-images shown in c) d) (red square) and e) f) (black square). The images c) and e) are from 2008. The images d) and f) are from 2009. Green stars indicates the boulders which have not moved, blue stars on 2008 images indicate the largest boulder which were taken away during the floods, red stars on 2009 images show the largest boulders which were deposited by the flood

Figures 5 a and b show a DEM and the associated orthorectified-image acquired by DRELIO during the 2008 campaign. These data cover a vegetated gravel bank and part of the river channel. The resolution of the DEM and of the orthoimage is around 3cm. The correlation of the two stereoscopic images is difficult under water. Moreover, the method used to compute the DEM does not take into account the optical effect of the water layer. This explains the poor quality of the DEM in the river. Some artifacts appear also where foam develops. Here again, the correlation produces bad results marked by unrealistic topographies. However the DEM on the gravel bank is precise and well defined as more than 90% of the points have been correlated. On the DEM, the trunk of the dead tree is clearly visible. Some points of the vegetated zones are clearly wrong but they remain rare.

The comparison of the gravel bank on the two orthoimages enables the observation of modifications of the granulometry and the morphology of the river bed between 2008 (Fig 5 c, e) and 2009 (Fig 5 d, f). The largest blocks, marked by a green star on figure 5, have not moved and are therefore visible on both images. Several smaller blocks have disappeared from the 2009 images. They have been taken away by floods that occurred between January 2008 and January 2009. The largest mobile blocks, which have a diameter of the order of 40 cm, are tagged with a blue star on figure 5. Finally, some blocks, not visible on the 2008 images, can be observed on the 2009 ones. The largest of these blocks, marked by a red star on Figure 5, have a maximum diameter of 1m. This image analysis does not provide direct measurement of bedload transport during an extreme event. The knowledge of both the size of the transported sediments and the hydrograph is however likely to provide important information on the dynamics of sediment transport that can be used to constrain bedload transport models.

6 DISCUSSION AND CONCLUSION

We have reported a methodology to estimate the impact of extreme events on sediment transport in rivers. Our approach relies on two complementary instruments developed and tested during a 1.5 years field survey performed from June 2007 to January 2009 on the Capesterre river located on Basse-Terre island (Guadeloupe archipelago, Lesser Antilles Arc). The first one, CAPMES, performs real-time in-situ measurements of the water level together with the concentration and the average grain size of suspended silts and sand particles. The second one, DRELIO, acquires high resolution images of river beds used to compute DEMs and to estimate how flash floods impact the granulometry and the morphology of the river.

These instruments have limitations. First of all, CAPMES is based on the use of a LISST-25X which operates in a volumetric concentration range going typically up to 100 ppm, corresponding to mass concentration of the order of a few g/L. This maximum concentration was never exceeded during our survey in Guadeloupe. However several authors have documented floods with suspended load concentrations reaching over 40 g/L, far above the limit of the LISST-25X (Dadson et al., 2005). A possibility to overcome that limit would be to implement an automatic dilution system designed to extend the concentration operating range. Similarly, the use of a LISST-100 instead of a LISST-25X would allow us to extend the resolution of the size distribution of suspended sediment from 2 to 32 logarithmically spaced size classes. We are currently exploring these possibilities.

Another problem comes from the fact that CAPMES cannot determine whether the suspended particles are terrigenous or organic. As a result, the concentration measured by CAPMES cannot be directly used to compute a sediment flux. To overcome that difficulty, we used an automatic water sampler (ISCO 6712) installed on the same site than CAPMES. This sampler is connected to a pressure gauge triggering acquisition. When a flood was detected, this instrument collected water with a rate of typically 1 sampling every 15 minutes and for a duration limited to 24 samples. The filtering and chemical analysis of the samples collected revealed that organic matter represented in average about 23% of the mass of suspended particles.

The DRELIO system has limitations in terms of images acquisition and of data processing. In the tropical zone, rivers are often bordered by a dense forest with high trees and branches overgrowing the channel at 5 to 10m height. DRELIO is not able to fly under the vegetation cover. Moreover the river is not visible when observed from 150m high. The river valley has to be at least 10m wide to be flown over and imaged in safe conditions. This limits the use of DRELIO in areas above the upper limit of the forest which is at around 1000m in Guadeloupe or in the alluvial part of the river where it is large enough.

The other limitation concerns the change of the river level for the different image acquisitions. The hydrological regime of Guadeloupean rivers is torrential and the water level is different for two acquisitions. As the images of the river bed which is under water are difficult to process, the data set is limited to the banks which are not covered by water. It is thus probable that the measurements of maximum size transported are underestimated. The maximum of the current is reached where the depth of river is maximum that is in the main stream which is under water even during the low water level conditions. One way to overcome this problem, is to develop mixed photogrammetric techniques able to take into account underwater data.

Despite these limitations, the combined use of CAPMES and DRELIO enables the acquisition of data sets that can be used to better constrain the dynamics of sediment transport during floods. They also

provide a platform of investigation of the erosive impact of extreme events easy to deploy in the field. We believe that this platform can be used either as part of a field campaign of limited duration, or within the frame of a long-term environmental survey of riverine transport.

7 ACKNOWLEDGEMENTS

We thank Y. Gamblin and A. Vieira for their technical assistance in designing and realizing CAPMES. We are indebted to O. Crispi, C. Antenor-Abazac, T. Kitou, P. Rival and the whole team of the Observatoire Volcanologique et Sismologique de Guadeloupe for their assistance on the field. We also strongly benefited from the assistance and expertise of Martial Pellegrinelli from the Direction Regionale de l'Environnement and from the agents of the "Parc National de la Soufrière de Guadeloupe". We thank Niels Hovius for his careful reading of the manuscript. We gratefully acknowledge support by the Agence Nationale de la Recherche through contract n° ANR-06-CATT-009-01 and by the "Agence Nationale de Valorisation de la Recherche" (ANVAR) which funded technical developments on DRELIO. This is IPGP contribution 3168.

REFERENCES

- Agrawal, Y. and Pottsmith, H. 2000, Instruments for particle size and settling velocity observations in sediment transport. *Marine Geology* 168, pp. 89-114.
- Burtin, A., L. Bollinger, J. Vergne, R. Cattin and J. L. Nábělek 2008, Spectral analysis of seismic noise induced by rivers: A new tool to monitor spatio-temporal changes in stream hydrodynamics, *J. Geophys. Res.*, 113, B05301, doi:10.1029/2007JB005034
- Burtin, A., L. Bollinger, R. Cattin, J. Vergne, and J. L. Nábělek 2009, Spatiotemporal sequence of Himalayan debris flow from analysis of high-frequency seismic noise, *J. Geophys. Res.*, 114, F04009, doi:10.1029/2008JF001198.
- Casson, B., Delacourt, C., and Allemand, P. (2005). Contribution of multi-temporal remote sensing images to characterize landslide slip surface ? Application to the La Clapiere landslide (France). *Natural Hazards and Earth System Science* 5, pp. 425-437.
- Chatanantavet, P., Lajeunesse, E., Parker, G., Malverti, L., and Meunier, P. (2010). Physically based model of downstream fining in bedrock streams with lateral input. *Water Resour. Res.* 46 : W02518, doi : 10.1029/2008WR007208.
- Chatanantavet, P., Parker, G., Lajeunesse, E., Planton, P., and Valla, P. (2007). Physically-based model of downstream fining in bedrock streams with side input and verification with field data. In Parker, G. and Garcia, editors, *River, Coastal and Estuarine Morphodynamics 2007*, pp. 571-579.
- Dadson, S., Hovius, N., Chen, H., Dade, W., Hsieh, M., Willett, S., Hu, J., Horng, M., Chen, M., Stark, C., et al. 2003, Links between erosion, runoff variability and seismicity in the Taiwan orogen, *Nature* 426(6967), pp. 648 - 651.
- Dadson, S., Hovius, N., Pegg, S., Dade, W., Horng, M., and Chen, H. 2005, Hyperpycnal river flows from an active mountain belt. *Journal of geophysical research*, 110(F4) :F04016.
- Delacourt, C., Allemand, P., Casson, B., and Vadon, H. 2004, Velocity field of the "la clapière" landslide measured by the correlation of aerial and quickbird images. *Geophys. Res. Lett.*, 31 :L15619.
- Delacourt, C., Allemand, P., Jaud, M., Grandjean, P., Deschamps, A., Ammann, J., Cuq, V. and Suanes, S. J. 2009, Drelío : An unmanned helicopter for imaging coastal areas. *Journal of Coastal research* 2 (Sp. Iss. 56), pp. 1489-1493.
- Feuillet, N., Manighetti, I., and Tapponnier, P. 2001, Extension active perpendiculaire : la subduction dans l'arc des petites antilles (Guadeloupe, antilles françaises) active arc-transverse normal faulting in Guadeloupe (French Lesser Antilles). *Comptes Rendus de l'Académie des Sciences-Series II A-Earth and Planetary Science*, 333(9) :583-590.
- Gabet, E., Burbank, D., Putkonen, J., Pratt-Sitaula, B. and Ojha, T. 2004, Rainfall thresholds for landsliding in the Himalayas of Nepal. *Geomorphology*, 63(3-4), pp.131-143.
- Gaillardet J., R. Setareh, K. Rivé, P. Louvat, C. Gorge, C.J. Allègre and E. Lajeunesse, Orography-driven chemical denudation in the Lesser Antilles: Evidence for a new feedback mechanism stabilizing atmospheric CO₂, submitted to *American Journal of science*
- Galy, A. and C. France-Lanord 2001, Higher erosion rates in the Himalaya: geochemical constraints on riverine fluxes, *Geology* 29, pp. 23-26
- Garcia, M. 2006. *ASCE Manual of Practice 110 Sedimentation Engineering : Processes, Measurements, Modeling, and Practice*. ASCE.
- Hilton, R., Galy, A., Hovius, N., Chen, M., Horng, M., and Chen, H. (2008). Tropical-cyclone driven erosion of the terrestrial biosphere from mountains, *Nature Geoscience* 1, pp. 759-762.
- Kasser, M. and Egels, Y. 2002, *Digital Photogrammetry*. Taylor and Francis : London.
- Kraus, K. and Waldhauser, P. 1994, 4th ed. *Photogrammetry, Fundamentals and Standard Processes*. vol. 1. Dümmler ISBN 3-427-78684-6.

- Lajeunesse E., L. Malverti & F. Charru, Bedload transport in turbulent flow at the grain scale: experiments and modeling, *J. Geophys. Res.*, 115, F04001, doi:10.1029/2009JF001628
- Lejot, J., Delacourt, C., Piegay, H., Fournier, T., Tremelo, M., and Allemand, P. 2007, Very high spatial resolution imagery for channel bathymetry and topography from an unmanned mapping controlled platform, *Earth surface Processes and Landforms* 32, pp.1705-1725.
- Lin, G., Chen, H., Hovius, N., Horng, M., Dadson, S., Meunier, P., and Lines, M. 2008, Effects of earthquake and cyclone sequencing on landsliding and fluvial sediment transfer in a mountain catchment, *Earth Surf. Proc. and Landforms* 33, pp. 1354-1373.
- Liu, Y., Metivier, F., Lajeunesse, E., Lancien, P., Narteau, C., and Meunier, P. 2008, Measuring bed load in gravel bed mountain rivers : averaging methods and sampling strategies. *Geodynamica Acta* 21, pp. 81-92.
- Melis, T., Topping, D., and Rubin, D. 2003, Testing laser-based sensors for continuous in situ monitoring of suspended sediment in the Colorado River, Arizona. In *Erosion and sediment transport measurement in rivers : Technological and methodological advances*, Proceeding of the Oslo workshop, june 2002, pp. 21-27.
- Meunier, P., Metivier, F., Lajeunesse, E., Meriaux, A. S., and Faure, J. 2006, Flow pattern and sediment transport in a braided river : The "torrent de st pierre" (french alps). *Journal of Hydrology* 330, pp. 496-505.
- Rad, S., Louvat, P., Gorge, C., Gaillardet, J., and Allegre, C. 2006, River dissolved and solid loads in the lesser antilles : New insight into basalt weathering processes, *Journal of Geochemical Exploration* 88, pp. 308-312.
- Samper, A., Quidelleur, X., Lahitte, P., and Mollex, D. 2007, Timing of effusive volcanism and collapse events within an oceanic arc island : Basse-terre, guadeloupe archipelago (lesser antilles arc). *Earth Planet. Sci. Lett.*, page doi :10.1016/j.epsl.2007.03.030.
- Sugiura, R., Noguchi, N., and Ishii, K. 2005, Remote-sensing technology for vegetation monitoring using an unmanned helicopter, *Biosystems engineering* 90, pp. 369-379.
- Summerfield, M. and Hulton, N. 1994, Natural controls of fluvial denudation rates in major world drainage basins. *J. Geophys. Res. - Solid Earth* 99(B7), pp. 13871-13883.
- Topping, D., Melis, T., Rubin, D., and Wright, S. (2004). High-resolution monitoring of suspended sediment concentration and grain size in the Colorado River in Grand Canyon using a laser-acoustic system. In *Proceedings of the Ninth International Symposium on River Sedimentation*, October, pp. 18-21.
- Turowski, J., Rickenmann, D., and Dadson, S. (2010). The partitioning of the total sediment load of a river into suspended load and bedload : a review of empirical data. *Sedimentology* 57, pp. 1126-1146.
- Wolman MG. 1954, A method for sampling coarse river-bed material, *American Geophysical Union Transactions* 35(6), pp. 951-956.